Mon. Not. R. Astron. Soc. **000**, 1–9 (1996) Printed 5 February 2008 (MN LATEX style file v1.4)

On the fundamental properties of dynamically hot galaxies

Alexei G. Kritsuk[1,2⋆]

[1] *Institute of Astronomy, University of St Petersburg, Stary Peterhof, St Petersburg 198904, Russia*
[2] *Max-Planck-Institut für Astrophysik, Postfach 1523, D-85740 Garching, Germany*

Accepted 1996 August 2. Received 1996 April 24; in original form 1995 October 18

ABSTRACT

A two-component isothermal equilibrium model is applied to reproduce basic structural properties of dynamically hot stellar systems immersed in their massive dark haloes. The origin of the fundamental plane relation for giant ellipticals is naturally explained as a consequence of dynamical equilibrium in the context of the model. The existence of two galactic families displaying different behaviour in the luminosity–surface-brightness diagram is shown to be a result of a smooth transition from dwarfs, dominated by dark matter near the centre, to giants dominated by the luminous stellar component. The comparison of empirical scaling relations with model predictions suggests that probably a unique dissipative process was operating during the violent stage of development of stellar systems in the dark haloes, and the depth of the potential well controlled the observed luminosity of the resulting galaxies. The interpretation also provides some restrictions on the properties of dark haloes implied by the fundamental scaling laws.

Key words: galaxies: elliptical and lenticular, cD – galaxies: formation – galaxies: fundamental parameters – dark matter

1 INTRODUCTION

The term 'dynamically hot galaxies' (DHGs) was introduced by Bender, Burstein & Faber (1992) for a class of stellar systems in which random motions provide most of the energy for support of the system. This class includes all varieties of elliptical galaxies from giant to dwarf and compact ellipticals, bulges of S0s and spirals, as well as dwarf spheroidal (dSph) galaxies.

High-quality photometric and spectral data accumulated for a large number of objects during the last decade, together with the application of more advanced methods of statistical analysis, provided empirical scaling laws that relate the global dynamical and structural observables of DHGs, namely the central velocity dispersion of stars σ_*, galaxy luminosity L, half-light radius R_e, and mean effective surface brightness $I_\mathrm{e} = L/2\pi R_\mathrm{e}^2$ (Kormendy & Djorgovski 1989; Djorgovski & de Carvalho 1990, and references therein). One of the possible representations of such a law for a sample of giant ellipticals (gEs) may be written as $L \propto \sigma_*^{3.45} I_\mathrm{e}^{-0.86}$ (Djorgovski & Davis 1987). Biparametric relations of this kind known as the fundamental plane (FP) indicate that the gEs populate a surface in a three-space of observables. Various projections of the surface reproduce correlations between the luminosity and central velocity dispersion known as the Faber–Jackson (1976) relation $L \propto \sigma_*^4$ (FJ) and between the surface brightness and the effective radius $\mu_\mathrm{e} \simeq 2.94 \log R_\mathrm{e} + const$ (HK), reported by Hamabe & Kormendy (1987). The bulges of early-type disc galaxies do not obviously deviate from the HK parameter correlation for ellipticals (Hamabe & Kormendy 1987).

While compact ellipticals follow nearly the same relations as the gEs, dwarf elliptical galaxies (dEs) form a separate family characterized by distinct scaling laws. They lie close to the FP for giant ellipticals but follow a different luminosity–surface-brightness relation $<\mu>_\mathrm{e} \simeq 0.75 M_B + const$ (Binggeli & Cameron 1991, hereafter BC). As far as the group of dwarf spheroidals is concerned, these galaxies also follow the uniparametric BC relation for dEs but deviate from the FP for gEs significantly (Bender et al. 1992; Burstein, Bender & Faber 1993).

The difference in the luminosity–surface-brightness relation for normal and dwarf ellipticals is supplemented with changes of galaxy surface brightness profiles along the galaxy sequence from giants, most of which are well described by the de Vaucouleurs $R^{1/4}$ empirical formula (see, e.g., Burkert 1993), to diffuse dwarfs and dSphs, which are better fitted by the exponential law (Faber & Lin 1983). These basic morphological features must be reproduced by any successful physical model of galaxy structure, formation and evolution.

There is extensive literature on the modelling, comprehensively reviewed by Ferguson & Binggeli (1994) and Gallagher & Wyse (1994) with emphasis on dwarf galaxies,

⋆ E-mail: agk@aispbu.spb.su

and by Kormendy & Djorgovski (1989), de Zeeuw & Franx (1991) and Burstein et al. (1993) for giant ellipticals. It is generally suggested that the properties of early-type galaxies are determined by dissipative collapse and then modified by mergers. The details of cooling, star formation, and feedback processes are considered to be important to produce the luminosity–surface-brightness relation (see references in the review papers above). However, each particular physical model usually contains a large number of free input parameters and therefore the interpretations do not appear to be unique.

One important source of uncertainties in the models is our poor knowledge of the nature and distribution of dark matter in DHGs (Kormendy 1988; Ashman 1992; Gallagher & Wyse 1994; de Zeeuw 1995). For spiral galaxies, flat H I rotation curves suggest the presence of extended isothermal dark haloes, and disc stability arguments support the idea that the dark halo has a spheroidal shape and, in any case, a much thicker distribution than the optical disc (Bertin & Stiavelli 1993). The detailed investigation of the main properties of the mass structure in spirals resulted in derivation of the 'universal rotation curve' – a counterpart to the FP of ellipticals (Persic, Salucci & Stel 1996). It shows two important features: (i) the distribution of dark matter in spirals is completely different from that of the luminous matter, and (ii) the dark matter content strongly and in a regular way depends on the luminosity, so that low-luminosity galaxies have much more *dark* matter than luminous matter, while luminous discs apparently dominate the internal dynamics of very high-luminosity systems. Until recently, neither observational nor theoretical arguments were sufficient to provide crucial evidence for the presence of dark matter in ellipticals (Bertin & Stiavelli 1993). However, if ellipticals were formed without dark haloes, the similarity between them and bulges of spirals would only be superficial (de Zeeuw & Franx 1991).

Combining the data on the inner ionized gas discs and on the H I discs extending to the outer regions of four elliptical galaxies, Bertola et al. (1993) showed that the variation of the mass-to-light ratio with galactocentric radius in ellipticals is qualitatively similar to that of spirals. Recent measurements of the shape of the stellar line-of-sight velocity distribution out to two effective radii in four elliptical galaxies provide definite evidence for the presence of massive dark haloes (Carollo et al. 1995). The mass profile for the elliptical galaxy NGC 4636, which is consistent with the stellar velocity dispersion and with *ROSAT* and *ASCA* X-ray temperature profiles, suggests that the galaxy becomes dark matter dominated at roughly the de Vaucouleurs radius (Mushotzky et al. 1994). A comparison of optical and X-ray mass determinations of galaxies, groups, and clusters of galaxies shows that most of the dark matter may reside in haloes around galaxies, typically extending to ~ 200 kpc for bright galaxies (Bahcall, Lubin & Dorman 1995). The haloes may be stripped off in the dense cluster environment to produce the suggested difference in scaling relations for field and cluster ellipticals (de Carvalho & Djorgovski 1992). Unlike giant ellipticals, some of the dwarf spheroidal galaxies have been found to show high *central* mass-to-light ratios (Aaronson & Olszewski 1987; Lake 1990; Mateo 1994; Armandroff et al. 1995; Vogt et al. 1995) that imply dSphs to be a class of dark matter dominated galaxies [note that there are alternative interpretations, e.g. Kuhn & Miller (1989)]. Thus the available data suggest that the abovementioned features of dark matter distribution in spirals may be relevant to the class of DHGs as well.

Obviously, the significant content of dark matter (either only in the halo region or all over the stellar system) will control the brightness profiles of the galaxies and therefore may play a major role in determining the observed global structural properties of DHGs. The purpose of this paper is to check whether or not the fundamental properties of DHGs can be explained solely as due to variations in dark matter content and spatial distribution in the galaxies. The preliminary answer is given here with the aid of an equilibrium galaxy model, which includes the stellar component and the dark component (both are isothermal, but with different temperatures) and which suggests the existence of a 'conspiracy' between the two following a simple power-law dependence, cf. Burkert (1994). Such a two-component model allows one to reconcile the dissipative effects (mainly related to the stellar, i.e. baryonic, component) with the dissipationless effects (related to the dark, presumably collisionless component) in the development of galaxies. Thus it may provide some hints about the initial conditions and the nature of star formation processes operating in DHGs.

The paper is organized as follows. Section 2 gives a detailed description of the model. Section 3 discusses the FP for giant ellipticals and the deviations of dSph galaxies from it as they originate in the context of the model. In Section 4 the distribution of DHGs in the luminosity–surface-brightness diagram is compared with the model predictions. The results are summarized in Section 5.

2 THE TWO-COMPONENT GALAXY MODEL

Let $M(r)$ be a spherically symmetric configuration of gravitating mass, including the stellar (luminous) component of a galaxy and its isothermal dark halo. The equilibrium dark matter distribution in a gravitational potential $\phi(r)$ of $M(r)$ can be described by

$$\sigma_{\rm DM}^2 \frac{\mathrm{d}\ \ln \rho_{\rm DM}}{\mathrm{d}\ \mathrm{r}} = -\nabla\phi \equiv -\frac{GM(r)}{r^2}. \tag{1}$$

The stellar density distribution of the galaxy, ρ_*, responding to the same gravitational potential, satisfies

$$\sigma_*^2 \frac{\mathrm{d}\ \ln \rho_*}{\mathrm{d}\ \mathrm{r}} = -\nabla\phi, \tag{2}$$

where $\sigma_{\rm DM}$ and σ_* are the one-dimensional velocity dispersions of dark matter particles and stars (it is assumed that both do not depend on the radius). The Poisson equation

$$\Delta\phi = 4\pi G(\rho_{\rm DM} + \rho_*) \tag{3}$$

closes the equation set. A set of four parameters ($\rho_{\rm DM,0}$, $\rho_{*,0}$, $\sigma_{\rm DM}$, and σ_*) completely defines the model.

It is straightforward to reduce the order of the system since the 'hydrostatic' dark matter and stellar densities are related via

$$\frac{\mathrm{d}\ \ln \rho_{\rm DM}}{\mathrm{d}\ \ln \rho_*} = \frac{\sigma_*^2}{\sigma_{\rm DM}^2} \equiv \beta, \tag{4}$$

or

$$\rho_{\rm DM} = \mathcal{C}\rho_*^{\beta}, \tag{5}$$

where $\mathcal{C}$ is the integration constant and β is the ratio of specific kinetic energies of stars and dark matter particles.

Given equation (5), one can determine the total mass distribution using the modified Poisson equation

$$\frac{1}{r^2}\frac{\mathrm{d}}{\mathrm{d}r}\left(r^2\frac{\mathrm{d}\ln\rho_*}{\mathrm{d}r}\right) = -\frac{4\pi G}{\sigma_*^2}(\rho_* + \rho_{\rm DM}). \quad (6)$$

Substituting dimensionless variables

$$x = r/r_0, \quad (7)$$

$$y = \rho_*/\rho_{*,0}, \quad (8)$$

where

$$r_0 = \frac{\sigma_*}{\sqrt{4\pi G\rho_{*,0}}}, \quad (9)$$

and introducing a new parameter as the ratio of the densities at the centre,

$$\delta = \rho_{\rm DM,0}/\rho_{*,0}, \quad (10)$$

one gets a generalized equation of Emden-Fowler type:

$$\frac{1}{x^2}\frac{\mathrm{d}}{\mathrm{d}x}\left(x^2\frac{\mathrm{d}\ln y}{\mathrm{d}x}\right) = -(y + \delta y^\beta). \quad (11)$$

It yields a biparametric family of solutions $y(x;\beta,\delta)$ for the initial conditions $y(0) = 1$, $y'(0) = 0$.

Now each particular model galaxy can be characterized by a pair of dimensional parameters (e.g., σ_* and r_0) that control the scaling, and a pair of dimensionless parameters β and δ that determine the shape of the light distribution in the galaxy. In this framework the structural homology generally assumed for the class of E galaxies implies the constancy of β and δ. Since there are indications that the homology is broken (see, e.g., Djorgovski 1995; Hjorth & Madsen 1995), all four parameters are treated as free in the following.

Parameter β defines the so-called 'conspiracy' of the dark and luminous matter. In the case of $\beta = 1$ the model describes a self-gravitating isothermal sphere of infinite mass with uniform mass-to-light ratio. A less concentrated dark matter distribution requires $\beta \in [0,\ 1)$. Asymptotically $\rho_* \sim r^{-2/\beta}$ when $r \to \infty$, and the mass of the stellar system is finite only for $\beta < 2/3$ if no tidal cut-off is introduced.

Parameter δ controls the dominant mass component in the centre of a galaxy, i.e. the galactic central mass-to-light ratio:

$$(M/L)_0 = \frac{\rho_{*,0} + \rho_{\rm DM,0}}{\rho_{*,0}(M/L)_*^{-1}} = (1+\delta)(M/L)_*; \quad (12)$$

here $(M/L)_*$ is the mass-to-light ratio of individual stars. Varying δ in the range from zero to ~ 100 one can cover the wide interval of M/L estimates based on observations of DHGs.

When $\beta = 1/2$ and $\delta \lesssim 0.1$, the stellar system has a density distribution of an isothermal sphere in the inner region and a cut-off at the core radius of the isothermal dark halo. In this case the density of luminous material varies as r^{-2} in the intermediate range of r outside the core region and asymptotically as r^{-4} in the outer region where the dark component dominates by mass. It is this behaviour that is required by the de Vaucouleurs surface brightness profile (Bertin & Stiavelli 1993). Figs 1–3 illustrate the variety of profiles responding to different values of δ and $\beta = 0.2, 0.5, 0.6$. While for $\delta \lesssim 0.1$ the profiles closely follow the empirical $R^{1/4}$ law in a range of radii $0.1R_{\rm e} \le r \le 1.5R_{\rm e}$ (Burkert 1993, 1994), they look more like exponential at $\delta \gtrsim 10$. The farther β deviates from 1/2, the worse fit the de Vaucouleurs formula yields in the limit of small δ. As a result the profiles generated for $\beta = 0.2$ or 0.6 do not satisfy the observational constraints on the quality of fit with the de Vaucouleurs formula established by Burkert (1993) who carried out a systematic analysis of CCD data for a large sample of E galaxies.

The physical meaning of the condition $\beta = 1/2$ can be readily understood in terms of a tentative dissipative galaxy formation scenario. When baryonic gas is initially thermalized in the dark halo potential well, its specific thermal energy equals the energy of dark matter particles and its density distribution follows that of the dark matter. If the efficiency of subsequent star formation follows the Schmidt law $\dot\rho_* \propto \rho_{\rm gas}^2$, the stellar density distribution will automatically satisfy the $\beta = 1/2$ condition. As the observed light profiles of gEs show a preference for such a choice of β, it will be considered as a working hypothesis hereafter.

The distributions of dark and luminous mass for $\delta = 0.01, 10$ and $\beta = 1/2$, typical for the model galaxies with (conventionally) 'de Vaucouleurs' and 'exponential' profiles, are shown in Figs 4(a) and 5(a). The mass of the stellar system is defined here as

$$\mathcal{M}_*(x) \equiv 4\pi\int_0^x x^2 y\mathrm{d}x. \quad (13)$$

The ratio of the total (dark+luminous) mass to $\mathcal{M}_*$ is given in Figs 4(b) and 5(b) to illustrate how the integral mass-to-light ratio depends on the radius. Note that when $\delta = 0.01$ the masses of stars and dark matter enclosed inside $R_{\rm e}$ are comparable (cf. Saglia, Bertin & Stiavelli 1992), but outside the half-light radius hidden matter dominates by mass that diverges $\sim r$ when $r \to \infty$. This inappropriate asymptotic behaviour does not significantly modify the global photometric quantities of the model galaxies, such as the luminosity or the mean effective surface brightness, while the value of β is not too close to 2/3. However, even for $\beta = 0.5$ and $\delta \lesssim 0.01$ the adopted isothermal approximation may result in a systematic overestimate of the luminosity by a factor of ~ 1.5, since the model predicts nearly perfect $R^{1/4}$ light profiles with no cut-off for radii up to $> 5R_{\rm e}$ (see Fig. 2), i.e. far outside the region typically covered by observations. The two-component self-consistent models of Bertin, Saglia & Stiaveli (1992), that take into account the effects of anisotropies expected to be present in both components, would be a better representation for real galaxies. Still, the isothermal model may be used as a zeroth-order approximation, since it is able to reproduce the general trend in global structural properties over the sequence of DHGs from giants to diffuse dwarf ellipticals.† The model suggests that the central mass-to-light ratio may indeed be the major parameter controlling the shape of light profiles of the galaxies. In order to find a range of realistic values of β and δ, one

† This model does not account for cluster-related phenomena, like the extended shells around cDs, which are beyond the scope of this paper.

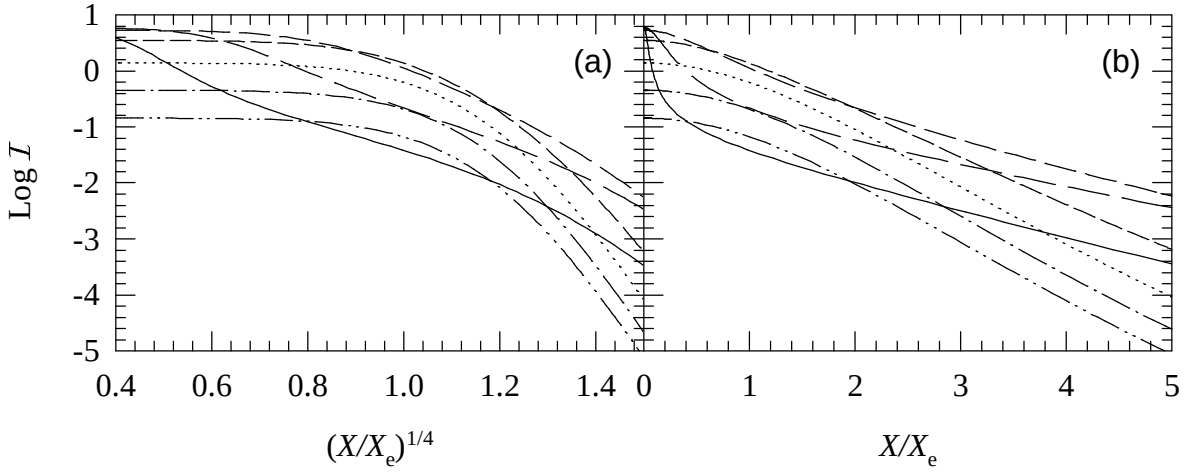

Figure 1. Simulated surface brightness profiles for $\beta = 0.2$. The sequence of line styles: solid, dashed (long, medium, short), dotted, dashed dotted, dashed double dotted corresponds to $\delta = 0.001, 0.01, 0.1, 1, 10, 100, 1000$, respectively. Panels (a) and (b), having different horizontal scales, display $R^{1/4}$ and exponential profiles as straight lines; radial distance X is given in units of the half-light radius X_e, see equation (15) below. The surface brightness $\mathcal{I}$ is given in dimensionless units defined by equation (17).

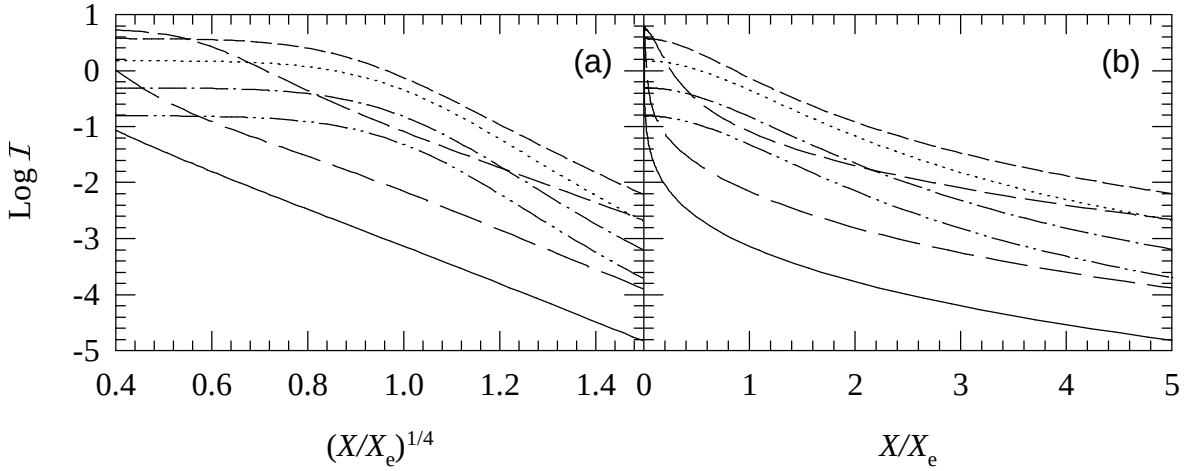

Figure 2. As Fig. 1 but for $\beta = 0.5$.

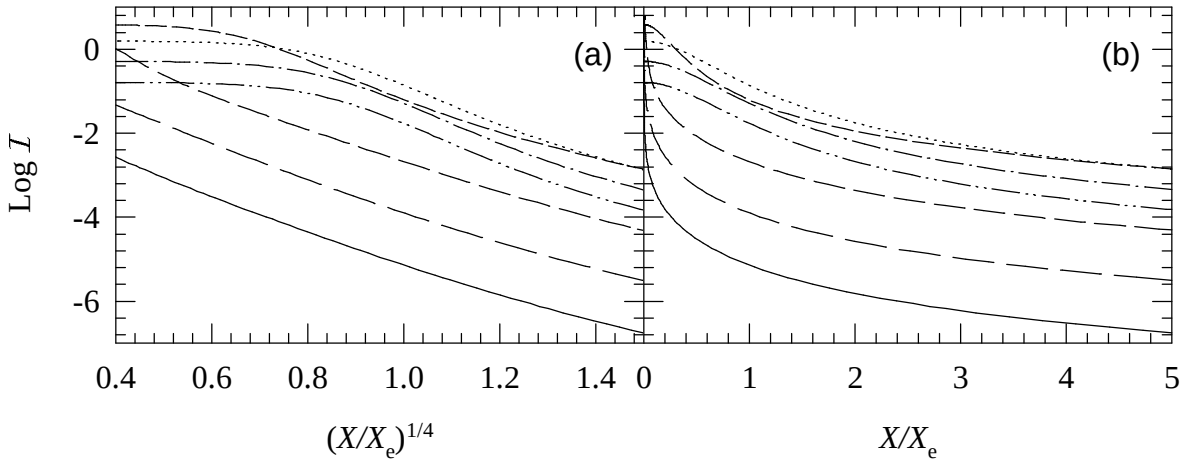

Figure 3. As Fig. 1 but for $\beta = 0.6$. Please note the difference in the ordinate scale compared with Figs 1 and 2.

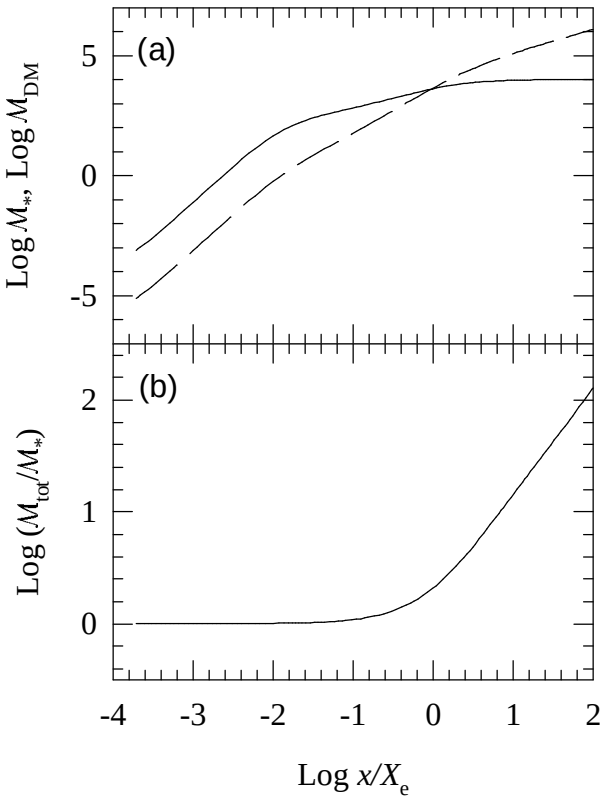

Figure 4. Mass of the luminous (solid line) and dark (dashed line) matter (panel **a**) and integrated mass-to-light ratio (panel **b**) versus radius for the model with $\beta = 0.5$ and $\delta = 0.01$.

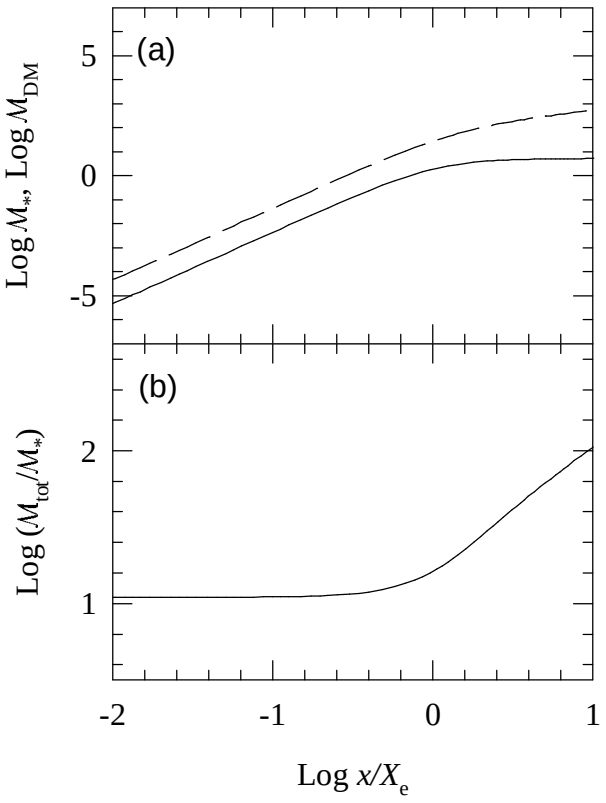

Figure 5. As in Fig. 4 but for $\delta = 10$.

should simulate the distribution of model galaxies in the 3D space of observables. This will be the subject of the following sections.

3 AN EDGE-ON VIEW OF THE FUNDAMENTAL PLANE

The fundamental plane for ellipticals is argued to contain clues to the initial conditions and processes of galaxy formation, being not just a consequence of the virial theorem. A simple reason behind this statement is that scale-free pure dynamics cannot explain the origin of the dimensional scaling laws (Bertin & Stiavelli 1993). If the existence of dark haloes is allowed, the homology hypothesis appears to be violated. Then a 'conspiracy' between the luminous and dark matter is able to introduce fractional power-law indices into the scale-free dynamical relationships and thereby into some of the observed correlations. This issue will be illustrated here with the aid of the two-component isothermal model.

Let $\mathcal{L}$, $X_{\rm e}$, and $\mathcal{I}_{\rm e}$ be *dimensionless* luminosity, half-light radius, and mean effective surface brightness, respectively, so that

$$\mathcal{L} \equiv \mathcal{M}_*(\infty) = \frac{4\pi G(M/L)_*}{r_0\sigma_*^2}L, \tag{14}$$

$$\mathcal{L}/2 = 2\pi \int_0^{X_{\rm e}} \mathcal{I}(X) X {\rm dX}, \tag{15}$$

$$\mathcal{I}_{\rm e} = \frac{\mathcal{L}}{2\pi X_{\rm e}^2}, \tag{16}$$

where

$$\mathcal{I}(X) \equiv 2\int_X^\infty \frac{yx{\rm dx}}{\sqrt{{\rm x}^2 - {\rm X}^2}} = \frac{4\pi G r_0 (M/L)_*}{\sigma_*^2} I(R) \tag{17}$$

is the dimensionless surface brightness and $X = R/r_0$ is the radial distance in projection.

These integral quantities can be readily calculated as functions of β and δ. In particular, for $\delta \gg 1$ the second term dominates in the *rhs* of equation (11), so the general solution can be approximated by the rescaled $y(\delta = 1)$ solution: $y(x;\beta,\delta) \approx y(x/\sqrt{\delta};\beta,1)$. The integral characteristics can be expressed as functions of δ explicitly:

$$\mathcal{I}(x,\delta) \approx \frac{\mathcal{I}(x,1)}{\sqrt{\delta}}, \tag{18}$$

$$X_{\rm e}(\delta) \approx \frac{X_{\rm e}(1)}{\sqrt{\delta}}, \tag{19}$$

and

$$\mathcal{L}(\delta) \approx \delta^{-\frac{3}{2}}\mathcal{L}(1), \tag{20}$$

where $\delta \gg 1$. At the other extreme, $\delta \lesssim 1$, there is no such simple analytical approximation owing to a more complicated restructuring of solutions, so a numerical technique has to be used.

In order to study the structural properties of dynamically hot galaxies, Bender et al. (1992) have defined an orthogonal coordinate system, which is termed as the κ-space:

$$\kappa_1 \equiv (\log \sigma_0^2 + \log R_\mathrm{e})/\sqrt{2}, \tag{21}$$

$$\kappa_2 \equiv (\log \sigma_0^2 + 2\log I_\mathrm{e} - \log R_\mathrm{e})/\sqrt{6}, \tag{22}$$

$$\kappa_3 \equiv (\log \sigma_0^2 - \log I_\mathrm{e} - \log R_\mathrm{e})/\sqrt{3}. \tag{23}$$

This coordinate system based on observables has been used to interpret the properties of DHGs in terms of known physical processes. The projection of galaxy distribution on the plane $\kappa_3 = const$ shows the FP close to face-on. In contrast, the $\kappa_1 = const$ and $\kappa_2 = const$ projections show two edge-on views of the FP. A major conclusion of Bender et al. (1992) was that all types of DHGs except the extreme dSphs lie nearly in the same FP as defined by the giant ellipticals.

While κ_1 and κ_2 coordinates are essentially dimensional, κ_3 is proportional to the central mass-to-light ratio (as follows from King's core-fitting formula) and can be expressed as a combination of the dimensionless variables defined above:

$$\kappa_3 = (\log X_\mathrm{e} - \log \mathcal{L} + const)/\sqrt{3}. \tag{24}$$

This allows for identification of a scale-free counterpart to the edge-on projection of the FP in terms of dimensionless variables $(\mathcal{I}_\mathrm{e}, \mathcal{L}, \delta)$, which is shown in Fig. 6. As the realistic range for δ is undefined at this stage, the graphs are given for a wide interval from 10^{-3} to 10^3; also for completeness three cases of β are shown. The asymptotics $\kappa_3 \sim const$ for $\delta \ll 1$ (the virial limit) and $\kappa_3 \sim (\log\delta + const)/\sqrt{3}$ for $\delta \gg 1$ [see the approximations (18)–(20)] are common to all represented values of β. In the intermediate range of δ ($-1.5 < \log\delta < 0.5$ for $\beta = 0.5$), where the solution undergoes a transition from one asymptotic behaviour to another, one can see a slight negative tilt ($\Delta\kappa_3 \simeq -0.1$) for $-1.5 < \log\delta < -0.2$, a minimum at $\delta \simeq -0.2$ and a rise at higher δ. These changes are implied by the non-trivial restructuring of the model galaxies in the course of the transition from luminous to dark matter dominated systems. If there is a one-to-one mapping between the luminosity (or 'the mass in the luminous confines' κ_1[‡]) and the dark matter content δ of DHGs, a comparison of the galaxy distribution in (κ_1, κ_3) projection [see fig. 1 from Burstein et al. (1993)] and the $\kappa_3 - \log\delta$ relation makes sense. The FP of gEs can be identified with a slightly tilted part of the $\beta = 0.5$ curve (cf. Renzini & Ciotti 1993; Ciotti, Lanzoni & Renzini 1996). Dwarf ellipticals, having progressively higher dark matter content, show small positive deviations from the FP. Finally, the dark matter dominated dSphs are characterized by extremely high mass-to-light ratios. If $\beta \simeq 0.5$ the deviations from the FP for gEs (roughly $\Delta\kappa_3 \simeq 1.1$ dex) demonstrated by the two most extreme dSph galaxies from the sample used in Burstein et al. (1993) correspond to $\delta \simeq 32$. Equation (12) then gives a central mass-to-light ratio of about $33(M/L)_*$, which is close to the values reported for Draco and Ursa Minor (Aaronson & Olszewski 1987; Lake 1990; Armandroff et al. 1995).

Thus the scale-free dependences implied by the two-component model are able to explain the gross features of edge-on projections for the distribution of DHGs about the FP for giant ellipticals. Similar analysis for the face-on view of the FP, which cannot be reduced to scale-free considerations, will be a subject of the following section.

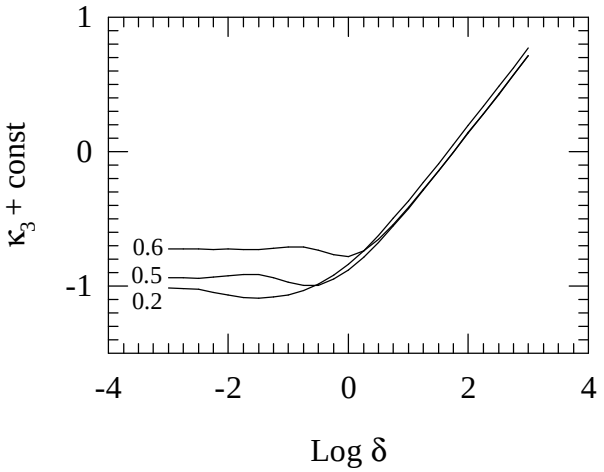

Figure 6. Plot of κ_3 versus δ for the grid of models with $\beta = 0.2, 0.5, 0.6$.

4 THE SYNTHETIC LUMINOSITY–SURFACE-BRIGHTNESS DIAGRAM

Within the FP, dynamically hot galaxies separate into two apparent sequences (Binggeli, Sandage & Tarenghi 1984; Kormendy 1985), which are clearly seen in the luminosity–surface-brightness diagram (see, e.g., Capaccioli, Caon & D'Onofrio 1992, 1993). The main sequence is defined by normal ellipticals (giant and intermediate), bulges, and compact ellipticals. Along this sequence, surface brightness decreases with growing luminosity. The second sequence is defined by dwarf ellipticals (nucleated and diffuse) and dwarf spheroidals (Bender et al. 1992; Burstein et al. 1993). The surface brightness grows with luminosity on this branch. A handful of compact ellipticals continue the main sequence towards lower luminosities beyond the turning point to the dwarf branch.[§]

The scale-free counterparts for the distribution of galaxies in the effective-radius–surface-brightness and luminosity–surface-brightness planes are shown in Figs 7(a) and (b). Plots of $\log\mathcal{I}_\mathrm{e}$ versus $\log X_\mathrm{e}$ and versus $\log\mathcal{L}$ are given for a grid of models with $\beta = 0.2, 0.5, 0.6$ and δ varying from 10^{-3} to 10^3. The curves $\beta = const$ display a characteristic shape of the empirical $R_\mathrm{e} - <\mu>_\mathrm{e}$ and $M_B - <\mu>_\mathrm{e}$ diagrams (Capaccioli et al. 1993, fig. 2), changing the sign of their slopes at $\delta \simeq 1$. However, a direct comparison of these scale-free diagrams with those based on observables is not possible since $L \propto r_0\sigma_*^2\mathcal{L}$, $I_\mathrm{e} \propto r_0^{-1}\sigma_*^2\mathcal{I}_\mathrm{e}$, and $R_\mathrm{e} \propto r_0 X_\mathrm{e}$, while r_0 and σ_* are unknown functions of δ. The major task

‡ Note that κ_1 was defined to represent roughly the mass of the galaxy 'within the luminous confines', assuming no rotational support and no structural variations among the galaxies.

§ This group of galaxies is assumed to have a specific formation history which controls their structural properties (see Burkert & Truran 1994), and therefore it stays outside the scope of this paper.

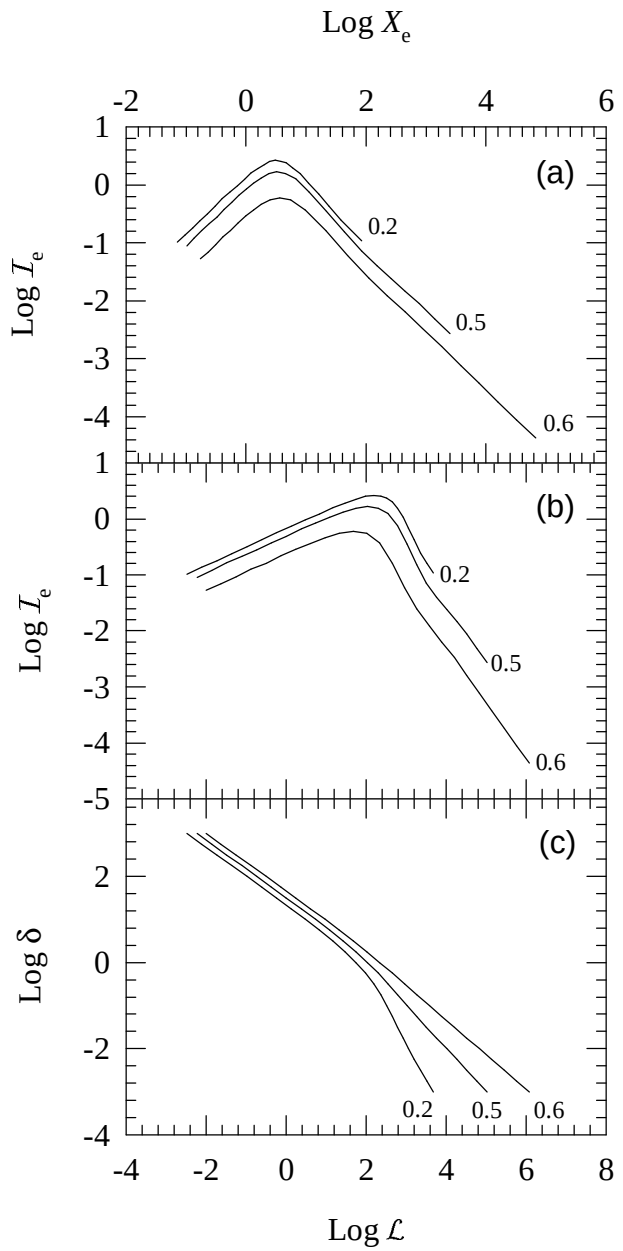

Figure 7. Global photometric quantities and the central dark-to-luminous mass density ratios for the set of models with $10^{-3} < \delta < 10^3$ and $\beta = 0.2, 0.5, 0.6$. (a) Mean effective surface brightness versus effective radius. (b) Mean effective surface brightness versus luminosity. (c) Central dark matter fraction δ versus luminosity. Note that axes are scaled in dimensionless units.

of this section is to determine these hidden parametric relationships (or their equivalents) and to delimit the range of realistic values of δ for the giant and dwarf branches separately.

Our considerations will be based on the following assumptions:

(i) the value of β is unique for both 'giant' and 'dwarf' families of galaxies;

(ii) $\beta \simeq 0.5$ since only in this case the model reproduces the $R^{1/4}$ brightness profiles of normal ellipticals;

Table 1. Power-law coefficients for the observed and simulated scaling relations.

Index	Giants		Dwarfs	
A	-0.86^1		1.33^2	
B	1.73^1		0	
C	2.0^3	1.2^4	2.0	2.8^5
D	-1.3^6	0.17^7	0.31^8	0.31^8
E	-1.0^6	-0.8^7	-0.7^8	-0.7^8
F	-0.52	-0.06	-0.40	-0.55
H	-1.04	-11.1	-1.6	-1.2

[1] The FP for giant ellipticals (Djorgovski & Davis 1987).
[2] The luminosity–surface-brightness relation for Virgo dwarfs (Binggeli & Cameron 1991).
[3] The Faber–Jackson (1976) relation.
[4] The luminosity–velocity-dispersion relation for dwarfs (Davies et al. 1983).
[5] As note 4 (Peterson & Caldwell 1993).
[6] The approximation for $\beta = 0.5$ and $\log\delta \in [-1.5,\ -0.5]$.
[7] As note 6, for $\log\delta \in [0,\ 0.5]$.
[8] As note 6, for $\log\delta \in [0,\ 3]$.

(iii) δ is the key quantity which traces the position of any particular galaxy in the three-space of observables;

(iv) the intersection point of the dwarf and giant branches coincides with a maximum in $\mathcal{I}_e(\mathcal{L})$ dependence.

This most straightforward approach to comparing the model with observations is not the only possibility. In particular, giant ellipticals are known to represent a biparametric family of galaxies and perhaps it cannot be described by varying only one dimensionless model parameter. However, the insights provided by the model are considered here only as indicating the direction for a more detailed study. Therefore, following the simplicity concept, the interpretation starts from the assumptions above.

Using power-law approximations for the observational scaling relations:

$$L \propto I_e^A \sigma_*^{2B}, \tag{25}$$

$$L \propto \sigma_*^{2C}, \tag{26}$$

and for the dependencies between the dimensionless quantities provided by the model (see Figs 7b and c):

$$\mathcal{I}_e \propto \mathcal{L}^D, \tag{27}$$

$$\delta \propto \mathcal{L}^E, \tag{28}$$

after some algebra one can show that if the model fits the observational relations then

$$\delta \propto L^F, \tag{29}$$

where

$$F = \frac{E(C + AC - B - 2A)}{AC(D+1)}. \tag{30}$$

The estimates for index values are given in Table 1. When F is known, the δ-scale can be calibrated in the luminosity units, which allows one to get rough estimates of the central dark-to-luminous mass density ratio for galaxies with known luminosity. With $F = -0.52$ the range of absolute magnitudes of gEs, $-25.5 < M_B < -19.5$ (Capaccioli et al.

1993), corresponds to a difference of ~ 1.3 dex in δ. The intersection point of two galaxy branches in the $(\mathcal{L}, \mathcal{I}_e)$ plane is located at $\log\delta \simeq -0.2$. Thus the brightest galaxies may have $\log\delta \simeq -1.5$, which means that they contain ~ 30 times more mass in stars than in dark matter in their core regions. At the same time, this range of δ confirms the suggested identification of the FP for gEs (see Section 3).

Note that a part of the mass that is conventionally termed here as 'dark' may be present in gEs as a hot gas emitting X-rays. The equilibrium density of this hot gas follows the dark matter distribution, and therefore fits the same model for the gravitational potential (with $\rho_{\rm gas} + \rho_{\rm DM}$ substituted for $\rho_{\rm DM}$). The typical ratio of the central stellar and hot gas densities for giant ellipticals estimated on the basis of the hydrostatic equilibrium model is $\sim 10^4$, so its contribution to δ must be negligible (Kritsuk 1996).

For dwarf galaxies the major source of uncertainty is the poorly known luminosity–velocity-dispersion relation [cf. Held et al. (1992) and Peterson & Caldwell (1993)], so three cases are represented in Table 1: the flat correlation $L \propto \sigma_*^{2.4\pm0.9}$ found by Davies et al. (1983), the much steeper dependence $L \propto \sigma_*^{5.6\pm0.9}$ suggested by Peterson & Caldwell (1993), and the luminosity–velocity-dispersion relation with the original FJ index. The observed range of luminosities of 4.6 dex from $M_B = -8$ to $M_B = -19.5$ implies the value of δ at the faint end of this branch to be roughly 2, 260, 60 for the three index values, respectively. Thus the normal FJ law gives an estimate of δ which is in rough agreement with the one determined in §3 for the extreme dSph galaxies of $M_V \simeq -9$.

The implemented fitting procedure also yields the index value H for the relation between the central stellar density and δ:

$$\rho_{*,0} \propto \delta^H, \tag{31}$$

$$H = \frac{(2C - A - 3AD - 2B - 2ACD)}{E(C + AC - B - 2A)} \tag{32}$$

(see Table 1). The value of $H \approx -1$ obtained for the giant branch implies a weak dependence of $\rho_{\rm DM,0}$ on δ along the gE sequence, cf. Kormendy (1988). In case of dwarf galaxies the uncertainties in F and H values are high due to the large spread of points in the (L, I_e) plane and the poorly determined value of C, but specifically steep luminosity–velocity-dispersion relations would roughly reproduce the scalings predicted by Dekel & Silk (1986) for their dark halo dominated model.

Undoubtedly, further observations are required to clarify the situation and only preliminary conclusions can be drawn at this stage, but it is not ruled out by the above analysis of the empirical scaling laws that both giant and dwarf galactic sequences are characterized by the same values of F and H.

In a special case when $F = -0.5$ and $H = -1$ the central stellar density and velocity dispersion would be related via $\rho_{*,0} \propto \sigma_*^2$ and the characteristic radius r_0 (which is proportional to the so-called King radius) would be a constant (see equation 9). Moreover, since it is assumed that $\beta = 1/2$, it follows from equations (4) and (5) that $\rho_*(r) \propto \rho_{\rm DM}^2(r)$ and $\sigma_*^2 = 0.5\sigma_{\rm DM}^2$. Therefore the distribution of stellar density in galaxies may be written as

$$\rho_*(r) = \left[8\pi G r_0^2 \rho_{\rm DM,0}^2\right]^{-1} \sigma_{\rm DM}^2 \rho_{\rm DM}^2(r), \tag{33}$$

where the expression in square brackets is a constant. Since $\sigma_{\rm DM}^2$ is related to the depth of the potential well, equation (33) implies that the initial burst of star formation (from baryonic gas thermalized in a potential of the dark halo) is regulated by a dissipative binary collisional process and the mass of the resulting stellar system is restricted (via the gradually increasing feedback heating) by the depth of the potential well. The final quasi-steady state which is observed can be reached either due to gas repulsion (winds driven by supernovae in the case of galaxies at the dwarf end) or due to gas consumption (the case of the giant end), and a combination of both may operate during the formation of intermediate ellipticals and bulges. Thus the ability to process baryonic gas into stars, controlled by the properties of dark haloes, provides the essential morphological features of DHGs.

This interpretation can hint at a coherent theory of dissipative galaxy formation, which must be able to reproduce the mass–luminosity-density–metallicity relation (Djorgovski & de Carvalho 1990; Matteucci 1992). The approach to such a theoretical scheme, however, requires details which must be considered elsewhere.

5 CONCLUSIONS

A two-component spherically symmetric galaxy model with a stellar system immersed in an isothermal massive dark halo has been applied to reconstruct basic properties of dynamically hot galaxies. While being obviously too crude to describe the observed detailed photometric and kinematical features (like isophote ellipticity and twisting, boxy and discy shapes, dynamically distinct dense nuclei, ripples and shells, etc.), the model reproduces the essence of changes in galaxy structure along the morphological sequence dSph–dE–gE (including bulges of S0 and spiral galaxies).

The conclusions of this study can be formulated as follows.

(i) Dark haloes of dynamically hot galaxies can play an important role in controlling the shape of their surface brightness profiles.

(ii) The existence of the fundamental plane for giant ellipticals and observed deviations of dwarf spheroidal galaxies from it follow naturally from the dynamical equilibrium condition in the framework of the two-component model.

(iii) The major difference in the empirical luminosity–surface-brightness relation for dwarf and giant families of galaxies could be explained in the context of a smooth transition from dark matter dominated dwarfs to luminous matter dominated (in the centre) giants.

(iv) The comparison of the model predictions with empirical scaling relations allows one to suggest that a common dissipative process operates during the initial violent stage of development of stellar systems in massive dark haloes of dwarf and giant galaxies. The outcome of the initial burst of star formation is regulated by the depth of the potential well of the galaxy halo.

These results should be considered as preliminary and indicating the direction for more detailed theoretical work. Also, new observations are necessary to define more exactly the scaling relations for dwarf galaxies.

ACKNOWLEDGMENTS

This work was partly supported by the Russian Foundation for Basic Research (project code 93-02-02957). The author is grateful to Bruno Binggeli, Massimo Persic and Massimo Stiavelli for useful comments on the manuscript, and to the staff of MPA for their warm hospitality.

REFERENCES

Aaronson M., Olszewski E., 1987, in Kormendy J., Knapp G.R., eds, Proc. IAU Symp. 117, Dark Matter in the Universe. Reidel, Dordrecht, p. 153
Armandroff T.E., Olszewski E.W., Pryor C., 1995, AJ, 110, 2131
Ashman K., 1992, PASP, 104, 1109
Bahcall N.A., Lubin L.M., Dorman V., 1995, ApJ, 447, L81
Bender R., Burstein D., Faber S.M., 1992, ApJ, 399, 462
Bertin G., Stiavelli M., 1993, Rep. Prog. Phys., 56, 493
Bertin G., Saglia R.P., Stiavelli M., 1992, ApJ, 384, 423
Bertola F., Pizzella A., Persic M., Salucci P., 1993, ApJ, 416, L45
Binggeli B., Cameron L. M., 1991, A&A, 252, 27 (BC)
Binggeli B., Sandage A., Tarenghi M., 1984, AJ, 89, 64
Burkert A., 1993, A&A, 278, 23
Burkert A., Truran J.W., 1994, in Hensler G., Theis Ch., Gallagher J., eds, Proc. International Scientific Spring Meeting of the Astron. Ges., Panchromatic View of Galaxies – their Evolutionary Puzzle. Editions Frontières, Gif-sur-Yvette, p.123
Burkert A.M., 1994, Reviews in Modern Astronomy, Vol. 7. Astronomische Gesellschaft, Hamburg, p. 191
Burstein D., Bender R., Faber S.M., 1993, in Danziger I.J., Zeilinger W.W., Kjär K., eds, Proc. ESO/EIPC Workshop, Structure, Dynamics and Chemical Evolution of Elliptical Galaxies. ESO, Garching, p. 31
Capaccioli M., Caon N., D'Onofrio M., 1992, MNRAS, 259, 323
Capaccioli M., Caon N., D'Onofrio M., 1993, in Danziger I.J., Zeilinger W.W., Kjär K., eds, Proc. ESO/EIPC Workshop, Structure, Dynamics and Chemical Evolution of Elliptical Galaxies. ESO, Garching, p. 43
Carollo C.M., de Zeeuw P.T., van der Marel R., Danziger I.J., Quian E., 1995, ApJ, 441, L25
Ciotti L., Lanzoni B., Renzini A., 1996, MNRAS, 282, 1
Davies R.L., Efstathiou G., Fall S.M., Illingworth G., Schechter P.L., 1983, ApJ, 266, 41
de Carvalho R.R., Djorgovski S., 1992, ApJ, 389, L49
de Zeeuw P.T., 1995, in van der Kruit P.C., Gilmore G., eds, Proc. IAU Symp. 164, Stellar Populations. Kluwer, Dordrecht, p. 215
de Zeeuw T., Franx M., 1991, ARA&A, 29, 239
Dekel A., Silk J., 1986, ApJ, 303, 39
Djorgovski S., 1995, ApJ, 438, L29
Djorgovski S., Davis M., 1987, ApJ, 313, 59
Djorgovski S., de Carvalho R., 1990, in Fabbiano G., Gallagher J.S., Renzini A., eds, Proc. Workshop of the Advanced School of Astronomy, Windows on Galaxies. Kluwer, Dordrecht, p. 9
Faber S.M., Jackson R.E., 1976, ApJ, 204, 668 (FG)
Faber S.M., Lin D.N.C., 1983, ApJ, 266, L17
Ferguson H.C., Binggeli B., 1994, A&AR, 6, 67
Gallagher J.S., III, Wyse R.F.G., 1994, PASP, 106, 1225
Hamabe M., Kormendy J., 1987, in de Zeeuw T., ed., Proc. IAU Symp. 127, Structure and Dynamics of Elliptical Galaxies. Reidel, Dordrecht, p. 379 (HK)
Held E.V., de Zeeuw T., Mould J., Picard A., 1992, AJ, 103, 851
Hjorth J., Madsen J., 1995, ApJ, 445, 55
Kormendy J., 1985, ApJ, 295, 73
Kormendy J., 1988, in Fang L.Z., ed., Proc. Guo Shoujing Summer School of Astrophysics, Origin, Structure and Evolution of Galaxies. World Scientific, Singapore, p. 252
Kormendy J., Djorgovski S., 1989, ARA&A, 27, 235
Kritsuk A.G., 1996, MNRAS, 280, 319
Kuhn J.R., Miller R.H., 1989, ApJ, 341, L41
Lake G., 1990, MNRAS, 244, 701
Mateo M., 1994, in Meylan G., Prugniel P., eds, Dwarf Galaxies. ESO Conference and Workshop Proceedings, No. 49, Dwarf Galaxies. ESO, Garching, p. 309
Matteucci F., 1992, ApJ, 397, 32
Mushotzky R.F., Loewenstein M., Awaki H., Makishima K., Matsushita K., Matsumoto H., 1994, ApJ, 436, L79
Persic M., Salucci P., Stel F., 1996, MNRAS, 281, 27 (also Erratum, MNRAS, 283, 000)
Peterson R.C., Caldwell N., 1993, AJ, 105, 1411
Renzini A., Ciotti L., 1993, ApJ, 416, L49
Saglia R.P., Bertin G., Stiavelli M., 1992, ApJ, 384, 433
Vogt S.S., Mateo M., Olszewski E.W., Keane M.J., 1995, AJ, 109, 151

This paper has been produced using the Royal Astronomical Society/Blackwell Science LaTeX style file.